Published in final edited form as:
Adv Healthc Mater. 2014 October ; 3(10): 1562–1567. doi:10.1002/adhm.201400051.

Nano-engineered particles for enhanced intra-articular retention and delivery of proteins

Prof. Ankur Singh,
Woodruff School of Mechanical Engineering, Georgia Institute of Technology, Atlanta, GA 30332, USA. Sibley School of Mechanical and Aerospace Engineering, Cornell University, Ithaca, NY 14853, USA

Dr. Rachit Agarwal,
Woodruff School of Mechanical Engineering, Georgia Institute of Technology, Atlanta, GA 30332, USA

Carlos A. Diaz-Ruiz,
Woodruff School of Mechanical Engineering, Georgia Institute of Technology, Atlanta, GA 30332, USA

Dr. Nick J. Willett,
Woodruff School of Mechanical Engineering, Georgia Institute of Technology, Atlanta, GA 30332, USA

Peiyi Wang,
Department of Chemistry and Biochemistry, University of South Carolina, Columbia, SC 29205, USA

Dr. L. Andrew Lee,
Department of Chemistry and Biochemistry, University of South Carolina, Columbia, SC 29205, USA. A&Q NanoDesigns, LLC., Columbia, SC 29201

Prof. Qian Wang,
Department of Chemistry and Biochemistry, University of South Carolina, Columbia, SC 29205, USA

Prof. Robert E. Guldberg, and
Woodruff School of Mechanical Engineering, Georgia Institute of Technology, Atlanta, GA 30332, USA. Petit Institute for Bioengineering and Bioscience, Georgia Institute of Technology, Atlanta, GA 30332, USA

Prof. Andrés J. García
Woodruff School of Mechanical Engineering, Georgia Institute of Technology, Atlanta, GA 30332, USA. Petit Institute for Bioengineering and Bioscience, Georgia Institute of Technology, Atlanta, GA 30332, USA

Andrés J. García: andres.garcia@me.gatech.edu

Correspondence to: Andrés J. García, andres.garcia@me.gatech.edu.

Keywords

nanoparticles; osteoarthritis; protein delivery; biomaterials

Osteoarthritis (OA) is the most common form of arthritis, affecting nearly 27 million Americans.[1] Epidemiological studies indicate that some evidence of OA can be found in 60% of the population over age 35, with radiographic evidence of cartilage thinning in more than 50% of adults over age 65.[2] OA is characterized by progressive degradation of cartilage, typically in load-bearing areas of one or more joints. Cellular changes include decreased chondrocyte viability and increased proliferation, altered matrix synthesis, and increased levels of pro-inflammatory cytokines such as interleukin (IL)-1β and tumor necrosis factor (TNF)-α, resulting in elevated production of matrix degrading enzymes and reactive oxygen species.[3],[4],[5] OA is often localized to joint spaces and therefore systemic delivery of OA-modifying drugs and therapeutics often results in poor improvement due to the lack of vascularity. Therefore localized intra-articular administration of drugs targeting cartilage or synovial inflammation has emerged as a promising strategy for therapeutic intervention in OA.[6],[7],[8] However, one of the major limitations with bolus small molecule and protein injections is the low retention within the intra-articular spaces. Upon intra-articular delivery, a drug is efficiently drained into lymphatics limiting residence times to as short as 1–2 hours.[6],[9] For example, Lornoxicam, an anti-inflammatory analgesic, leaks quickly into the systemic circulation and therefore has a short residence time (< 48 hours) and half-life in the joint. To achieve prolonged release and retention of therapeutics in the intra-articular space, biomaterials-based formulations such as hydrogels, liposomes, and polymeric micro/nano-particles have been reported. Compared to the bolus injections of drug itself, Lornoxicam-encapsulated poly(lactic-co-glycolic acid) (PLGA) microparticles have prolonged the retention in healthy rat joint to 96 hours.[10] Large gelatin microparticles (~ 70 μm) have also been examined to deliver basic fibroblast growth factor in healthy rabbit joints, however only 3% protein was retained in the joint cavity after 7 days.[11] Whereas many of these drug delivery vehicles demonstrate reductions in inflammation, their applicability is severely limited by suboptimal drug dosing kinetics and biostability as well as inadequate mechanical and biological properties. For instance, many of these polymeric materials (e.g., PLGA) elicit non-specific inflammatory responses and are limited in the encapsulation/delivery of proteins. Similarly, liposome carriers have poor stability and release kinetics. We are particularly interested in nanoparticles because the nanoscale dimension: (i) provides for increased retention of the carrier in the joint;[12],[13],[14] (ii) is smaller than micron-sized particles that are phagocytosed by resident cells and elicit inflammation;[12] and (iii) allows simple delivery via intra-articular injections for local administration. Various nanoparticles-based systems have been developed for delivery of therapeutic drugs to the joint.[15],[16],[17],[18],[19],[20],[21] We recently reported self-assembling nanoparticles presenting interleukin-1 receptor antagonist (IL-1Ra) for enhanced delivery, retention, and bioactivity in the OA joint.[22] These 300 nm nanoparticles demonstrated significantly longer retention time for IL-1Ra in the rat stifle joint compared to that of soluble IL-1Ra and no adverse effect on the cartilage structure in the joint. We then hypothesized that larger sized nanoparticles in the 500–1000 nm range will prolong the retention of proteins in rat intra-articular stifle joint space. Although previously reported

nanoparticles were promising delivery vehicles, we were limited in our ability to engineer variable size particles. Here, we report a new class of self-assembly polymer which contains a poly-hydroxyethylmethacrylate (pHEMA) backbone with a functionalized hydrophobic side chain of pyridine to vary the particle size range (Figure 1A) and demonstrate the effect of nanoparticle size on protein retention time in the rat intra-articular stifle joint space.

pHEMA-pyridine was synthesized by reacting pHEMA with nicotinoyl chloride hydrochloride in tetrahydrofuran and pyridine as indicated in Figure 1B. Post purification, a white solid was recovered with 51% yield and the resulting modified pHEMA was confirmed by ^{1}H NMR as indicated in Figure 1C (300 MHz, $CDCl_3$, ppm): 9.13 (1H, pyridine-H), 8.17 (1H, pyridine-H), 8.23 (1H, pyridine-H), 7.38 (1H, pyridine-H), 4.48 (2H, OCH_2), 4.22 (2H, OCH_2), 1.80 (2H, CH_2), 0.89–1.01 (3H, CH_3).

To incorporate biotherapeutics such as proteins, the modified polymer was incubated with the target biomolecule in aqueous buffer (Fig. 1A). This tethering approach overcomes major limitations of other biomaterial carriers that require organic solvents that affect therapeutic protein activity or multi-step chemical reaction procedures. Similar to our previous work in constructing polymer-virus core-shell nanoparticles,[23],[24],[25] the protein-polymer complexation is very fast and the resulted nanoparticles can be simply washed and collected by centrifugation. In the present work, we focused on tethering the model protein bovine serum albumin (BSA) and a therapeutic targeting ligand fibronectin onto the self-assembling nanoparticles. The polymer assembled into nanoparticles with average diameters that depended on the protein:polymer ratio of the reactants. By keeping the polymer amount at 0.4 mg (2.0 mg mL^{-1}, 0.2 mL), increasing the amount of BSA protein was able to modulate the size of nanoparticles. As seen in Figure 2A and B, the 2:1 ratio resulted in spherical particles with an average diameter of 303±13 nm and the 1.875:1 ratio yielded nanoparticles of 500 ± 22 nm average diameter. The largest diameter size corresponds to the 1.5:1 ratio nanoparticle (910 ± 46 nm) suggesting an increase in particle size with decrease in protein content.

Although we observed nearly 100% modification of pyridine, the polymer still retains its more hydrophilic parts, i.e. the arms and the nicotinoyl groups which are more hydrophilic in comparison with the main methacrylate chain. Therefore the resulting polymer is more hydrophobic than pHEMA. We hypothesize that the assembly process is primarily entropically driven, with electrostatic interaction and hydrogen bonding as “patches” to stabilize the final structures. The displacement of proteins (serving as pseudo-amphiphiles) between the interface of water and pHEMA-pyridine, which is insoluble at a pH > 5, can minimize the interfacial energy, a similar process as the formation of Pickering emulsions.[26],[27] On the other hand, an optimal polymer structure is critical for a successful assembly since it provides a hydrophobic nature to drive the assembly while the pyridinyl units can form hydrogen-bonds with proteins and create a benign microenvironment to assist the conformational preservation of proteins.

One major concern for our application is the stability of the protein-shell of the assembled complex against serum proteins. Hence we evaluated the aggregation and stability of nanoparticles in serum-containing media. As indicated by dynamic light scattering (Figure

2C), the nanoparticles with 900 nm initial diameter maintained their size over a period of 2 weeks suggesting serum stability and minimal aggregation. Similar stability results were obtained from smaller size nanoparticles (500 nm) over a period of 14 days. We next performed material cytotoxicity studies by incubating RAW 264.7 macrophage cells with increasing doses of nanoparticles (0.2 – 2.0 mg/mL) and observed no cytotoxic effects on the cells over a period of 24 hours (Figure 2D).

We next assessed the ability to form nanoparticles with human fibronectin (FN) protein which has a different molecular weight than BSA and has merit as a therapeutic targeting ligand.[28],[29] Similar to BSA nanoparticles, we successfully generated 200 nm nanoparticles using human plasma fibronectin (FN-NPs, Figure 2E) at 2:1 protein to polymer ratio. All nanoparticle samples had a narrow size distribution with polydispersity index (PDI) in the range of 0.13 – 0.29. We did not observe any influence of nanoparticle size or protein type (BSA vs fibronectin) on PDI.

To assess the bioactivity of FN-NPs, we used the monoclonal antibody HFN7.1 against human fibronectin that binds in the cell binding domain of fibronectin. Importantly, we previously demonstrated that this antibody is receptor-mimetic and serves as an excellent surrogate of integrin-mediated cell adhesion.[30] An irrelevant mouse antibody that does not bind to human fibronectin and BSA-NPs were used as controls. HFN7.1 antibody demonstrated significantly higher binding FN-NPs compared to BSA-NPs ($p<0.0001$), and this binding was specific to the HFN7.1-FN interaction as a IgG control antibody had background binding levels (Figure 2E). Our results clearly demonstrates that this is a generalizable approach to form protein loaded nanoparticles and the loaded protein retains bioactivity.

Finally, we assessed the role of nanoparticle size in prolonged retention in the intra-articular space in the rat stifle joint. We have previously used *in vivo* fluorescence imaging to monitor delivery of therapeutic proteins labeled with near-IR dyes.[22],[31] This strategy provides a simple and powerful approach to measure delivery/retention profiles over time in the same cohort of subjects. Endotoxin-free BSA was conjugated with VivoTag®-S 750, an amine-reactive near-IR fluorochrome, and nanoparticles were prepared as described earlier. Using fluorescence molecular tomography, we evaluated the relationship between size of the nanoparticles and retention time in rat intra-articular stifle joint space.

As seen on Figure 3, soluble protein exhibited poor retention in the joint with a half-life of 0.63 days. Both 500 and 900 nm particles demonstrated significantly longer retention of protein ($p<0.025$ and $p<0.05$, respectively) compared to soluble protein. The BSA-complexed 500 nm nanoparticles exhibited a half-life of 1.9 days whereas the larger nanoparticles (900 nm) exhibited a longer half-life of 2.5 days. Importantly, 900 nm particles exhibited sustained retention (~30% at 14 days) compared to the 500 nm particles and soluble protein, indicating an improvement in prolonged retention using larger size nanoparticles within the intra-articular joint space. Conventionally, high concentration of a drug is administered at the OA joint and despite lacking vasculature, soluble drugs can easily drain through the trans-synovial flow into the lymphatics and to the circulation. Localized delivery of larger size nanoparticles with longer retention time in the joint

represents a promising strategy to target the disease site of OA development potentially eliminating the need for large and repeated doses of therapeutics. In addition, such systems are highly useful for targeted delivery of therapeutics, such as IL-1Ra, as they provide longer exposure time for ligand-receptor interactions between the nanoparticles and IL-1 secreting synoviocytes. Future studies will focus on studying the retention of IL-1Ra protein in rat knee and treatment of OA in rats with induced knee injuries. Our *in vivo* results, in combination with the *in vitro* protein stability data, suggests that the protein remains coupled to the nanoparticle for at least 14 days. Further in vivo studies are necessary to establish longer tissue retention and any disintegration of protein-nanoparticle complexes beyond 14 days.

Intra-articular drug delivery is the most direct route for administering drugs and proteins for arthritis and other joint disorders. However, many of the polymeric materials (e.g., poly(lactic-co-glycolic) acid) used for delivery elicit non-specific inflammatory responses and are limited in the encapsulation/delivery of proteins. A major limitation of localized delivery is rapid clearance from the intra-articular space. Using protein-polymer complexes at different weight ratios, we have engineered particles of 500 and 900 nm size and demonstrated prolonged retention with larger nanoparticles compared to smaller nanoparticles and bolus protein over a period of 14 days. In addition to the protein:polymer ratio, we expect that the length and extent of substation of the polymer are important parameters controlling the size of the resulting nanoparticles. In this study, we did not observed a significant effect of protein molecular weight or type on the size of the resulting nanoparticles. Localized delivery of larger size nanoparticles with longer retention time in the joint represents a promising strategy to target the disease site of OA development without the need for large and repeated doses of therapeutics. We demonstrate the use of therapeutic targeting ligand fibronectin, suggesting the use of nanoparticles for targeted delivery approaches. Finally, these particles can have a wide range of applications for protein, peptides, and other therapeutic delivery to treat inflammation, diseases like infections and cancer, and regenerate tissues.[32],[29],[33],[34],[10]

Experimental Section

Synthesis of pHEMA-pyridine

Poly(2-hydroxyethyl methacrylate) (MW 20K, 0.13 g, 1.0 mmol -OH equiv.) and nicotinoyl chloride hydrochloride (0.21 g, 1.2 mmol) were dissolved in THF (4 mL) and pyridine (2 mL). After the mixture was stirred at room temperature for 24 h, the solvents were removed under reduced pressure, and then the crude mixture was redissolved in dichloromethane. The organic layer was washed by water, brine and dried with anhydrous sodium sulfate. The solution was concentrated under reduced pressure until the final volume reached 1 mL; and then it was added dropwise to cold ethyl ether.

Nanoparticle preparation and characterization

A solution of pHEMA-pyridine in dimethylformamide (DMF) (2.0 mg mL^{-1}, 0.2 mL) was slowly added to a solution of endotoxin-free BSA protein (0.60 mg for 900 nm particle and 0.75 mg for 500 nm particles) in PBS buffer (5 mL) while vortexing it gently. The volume

percentage of DMF was less than 5%. The mixtures were dialyzed against water for 24 h. Particle stability tests were performed to assess the potential of particles to agglomerate under serum conditions (1% fetal bovine serum (FBS)) over a period of 14 days. At each time point (1, 4, 7, and 14 days), particle sizes were measured using a Brookhaven 90 Plus Particle Size analyzer. The 1% FBS was filtered using a 40 μm cell strainer to eliminate large size clusters of serum proteins that might interfere with the nanoparticle size readings. For scanning electron microscopy (SEM), nanoparticle suspension (5 μL) was dispensed on a SEM stub, air dried for 2 hours and sputter coated with 5 nm of gold to make the sample conductive. Imaging was done with a 5 KeV electron beam.

To engineer human plasma fibronectin-loaded nanoparticles, a solution of pHEMA-pyridine in dimethylformamide (DMF) (2.0 mg mL^{-1}, 0.3 mL) was slowly added to a solution of human fibronectin (1.2 mg) in PBS buffer (5 mL) while vortexing it gently. For functional assay, nanoparticles (0.4 mg fibronectin or BSA particles) were suspended in PBS (1 mL) and HFN7.1 mouse antibody (Developmental Hybridoma Studies Bank, 2 μg/mL) or a non-specific IgG control mouse antibody (2 μg/mL) was added and incubated for 1 hr at room temperature. Particles were then washed twice with PBS by centrifugation and then incubated in Alexa Fluor 488-conjugated anti-mouse IgG antibody (2 μg/mL). Particles were washed twice with PBS and fluorescence readings were taken using a Perkin-Elmer HTS 7000 plate reader.

Cytotoxicity assay

RAW 264.7 macrophage cells (ATCC, Manassas, VA) were cultured in Dulbecco's Minimum Essential Media (DMEM) supplemented with 10% FBS at 37°C, 5% CO_2. Cells (10,000) were seeded on a 96-well tissue culture treated plastic surface and allowed to adhere overnight. *In vitro* cytotoxicity assay was performed using a cell metabolic activity assay (CellTiter 96 AQueous One Solution Cell Proliferation Assay, Promega). Assays were performed by adding the reagent solution to culture wells and recording the absorbance (490 nm) at after particle incubation of 24 hr. All the experiments were done in groups of 6.

Intra-articular delivery and retention

All procedures were approved by Georgia Tech's Institutional Animal Care and Use Committee. Endotoxin-free BSA was conjugated with VivoTag®-S 750 per the manufacturer's protocol. Male Lewis rats (10–12 week old, n = 5) received either particles or soluble protein (50 μL, 500 μg VivoTag®-S 750-BSA) via an intra-articular injection to the right stifle joint space, while the left stifle received the equivalent volume of saline and served as a contralateral control. Rats were deeply anesthetized with isofluorane. The hair was removed from the hind limb surgical sites and the skin, and injections were delivered to the intra-articular space by palpating the patellar ligament below the patella and injecting the particle solution through the infrapatellar ligament using a sterile 27-gage 0.5″ needle. Subjects were fully ambulatory following recovery and all injections were well tolerated. Animals receiving particles or soluble protein were scanned in Fluorescence Molecular Tomography imaging system (Perkin Elmer). Fluorescence intensity was measured as background-subtracted average efficiency within a region of interest centered on the knee. Intensity values over time were analyzed using FMT software. At the end point of the study,

rats were euthanized by CO_2 inhalation. Data from each animal were normalized to their individual day 0 values. The normalized data were fitted using a one-phase exponential decay using GraphPad Prism 5.0 (GraphPad Software, La Jolla, CA, USA).

Acknowledgments

This work was supported by the Arthritis Foundation and the NIH (P20 HL113451). QW is thankful to the financial support of US NSF CHE-1307319.

References

1. Helmick CG, Felson DT, Lawrence RC, Gabriel S, Hirsch R, Kwoh CK, Liang MH, Kremers HM, Mayes MD, Merkel PA, Pillemer SR, Reveille JD, Stone JH. Arthritis Rheum. 2008; 58:15. [PubMed: 18163481]
2. Peyron JG. Semin Arthritis Rheum. 1979; 8:288. [PubMed: 382362]
3. Bonnet CS, Walsh DA. Rheumatology (Oxford). 2005; 44:7. [PubMed: 15292527]
4. Pelletier JP, Martel-Pelletier J, Abramson SB. Arthritis Rheum. 2001; 44:1237. [PubMed: 11407681]
5. Brandt KD, Dieppe P, Radin E. Med Clin North Am. 2009; 93:1. [PubMed: 19059018]
6. Rothenfluh DA, Bermudez H, O'Neil CP, Hubbell JA. Nature materials. 2008; 7:248.
7. Bondeson J. Curr Drug Targets. 2010; 11:576. [PubMed: 20199392]
8. Bondeson J, Blom AB, Wainwright S, Hughes C, Caterson B, van den Berg WB. Arthritis Rheum. 2010; 62:647. [PubMed: 20187160]
9. Owen SG, Francis HW, Roberts MS. Br J Clin Pharmacol. 1994; 38:349. [PubMed: 7833225]
10. Zhang Z, Huang G. Drug Deliv. 2012; 19:255. [PubMed: 22775466]
11. Inoue A, Takahashi KA, Arai Y, Tonomura H, Sakao K, Saito M, Fujioka M, Fujiwara H, Tabata Y, Kubo T. Arthritis and rheumatism. 2006; 54:264. [PubMed: 16385543]
12. Liggins RT, Cruz T, Min W, Liang L, Hunter WL, Burt HM. Inflamm Res. 2004; 53:363. [PubMed: 15316667]
13. Horisawa E, Hirota T, Kawazoe S, Yamada J, Yamamoto H, Takeuchi H, Kawashima Y. Pharm Res. 2002; 19:403. [PubMed: 12033371]
14. Horisawa E, Kubota K, Tuboi I, Sato K, Yamamoto H, Takeuchi H, Kawashima Y. Pharm Res. 2002; 19:132. [PubMed: 11883639]
15. Williams AS, Topley N, Dojcinov S, Richards PJ, Williams BD. Rheumatology (Oxford). 2001; 40:375. [PubMed: 11312373]
16. Butoescu N, Seemayer CA, Foti M, Jordan O, Doelker E. Biomaterials. 2009; 30:1772. [PubMed: 19135244]
17. Bendele A, McAbee T, Woodward M, Scherrer J, Collins D, Frazier J, Chlipala E, McCabe D. Pharm Res. 1998; 15:1557. [PubMed: 9794498]
18. Boza A, Caraballo I, Alvarez-Fuentes J, Rabasco AM. Drug Dev Ind Pharm. 1999; 25:229. [PubMed: 10065357]
19. Moriuchi-Murakami E, Yamada H, Ishii O, Kikukawa T, Igarashi R. J Rheumatol. 2000; 27:2389. [PubMed: 11036835]
20. Kim WU, Lee WK, Ryoo JW, Kim SH, Kim J, Youn J, Min SY, Bae EY, Hwang SY, Park SH, Cho CS, Park JS, Kim HY. Arthritis Rheum. 2002; 46:1109. [PubMed: 11953991]
21. Knight CG, Shaw IH. Front Biol. 1979; 48:575. [PubMed: 387470]
22. Whitmire RE, Wilson DS, Singh A, Levenston ME, Murthy N, Garcia AJ. Biomaterials. 2012; 33:7665. [PubMed: 22818981]
23. Li T, Niu Z, Emrick T, Russell TP, Wang Q. Small. 2008; 4:1624. [PubMed: 18819135]
24. Li, T.; Wu, L.; Suthiwangcharoen, N.; Bruckman, MA.; Cash, D.; Hudson, JS.; Ghoshroy, S.; Wang, Q. Chemical communications. 2009. p. 2869
25. Li T, Ye B, Niu Z, Thompson P, Seifert S, Lee B, Wang Q. Chem Mater. 2009; 21:1046.

26. Niu Z, He J, Russell TP, Wang Q. Angew Chem Int Ed Engl. 2010; 49:10052. [PubMed: 21161962]
27. Russell JT, Lin Y, Boker A, Su L, Carl P, Zettl H, He J, Sill K, Tangirala R, Emrick T, Littrell K, Thiyagarajan P, Cookson D, Fery A, Wang Q, Russell TP. Angew Chem Int Ed Engl. 2005; 44:2420. [PubMed: 15806611]
28. Yoder MC. Clin Perinatol. 1991; 18:325. [PubMed: 1879111]
29. Schaffner F, Ray AM, Dontenwill M. Cancers (Basel). 2013; 5:27. [PubMed: 24216697]
30. Keselowsky BG, Collard DM, Garcia AJ. Journal of biomedical materials research Part A. 2003; 66:247. [PubMed: 12888994]
31. Phelps EA, Landazuri N, Thule PM, Taylor WR, García AJ. Proc Natl Acad Sci U S A. 2010; 107:3323. [PubMed: 20080569]
32. Rothenfluh DA, Bermudez H, O'Neil CP, Hubbell JA. Nat Mater. 2008; 7:248. [PubMed: 18246072]
33. Singh A, Nie H, Ghosn B, Qin H, Kwak LW, Roy K. Mol Ther. 2008; 16:2011. [PubMed: 18813280]
34. Singh A, Qin H, Fernandez I, Wei J, Lin J, Kwak LW, Roy K. Journal of controlled release: official journal of the Controlled Release Society. 2011; 155:184. [PubMed: 21708196]

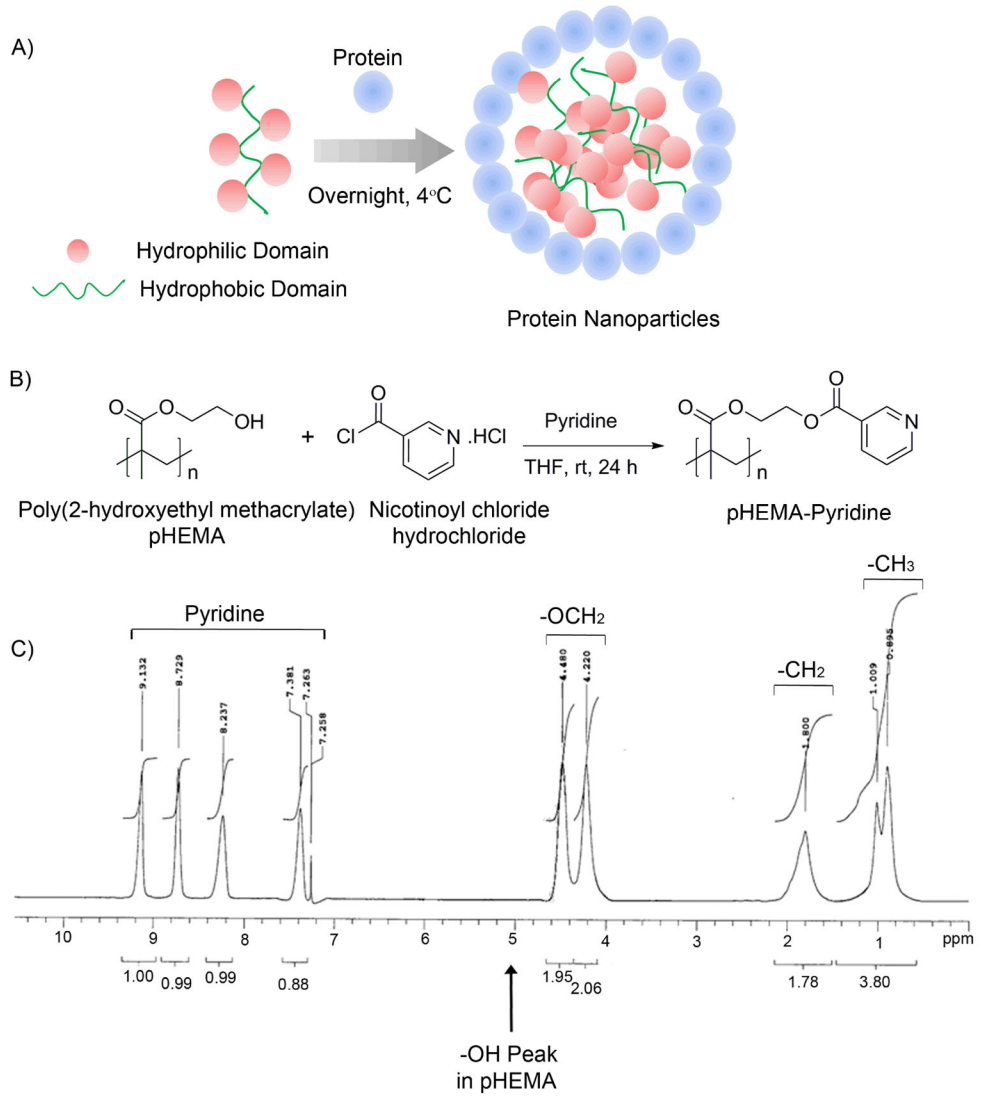

Figure 1. Protein complexed pHEMA-pyridine nanoparticles

A) Schematic of nanoparticle self-assembly based on protein/polymer complexation. B) pHEMA-pyridine was synthesized by reacting pHEMA with nicotinoyl chloride hydrochloride in tetrahydrofuran and pyridine. C) pHEMA modification was confirmed by ^{1}H NMR.

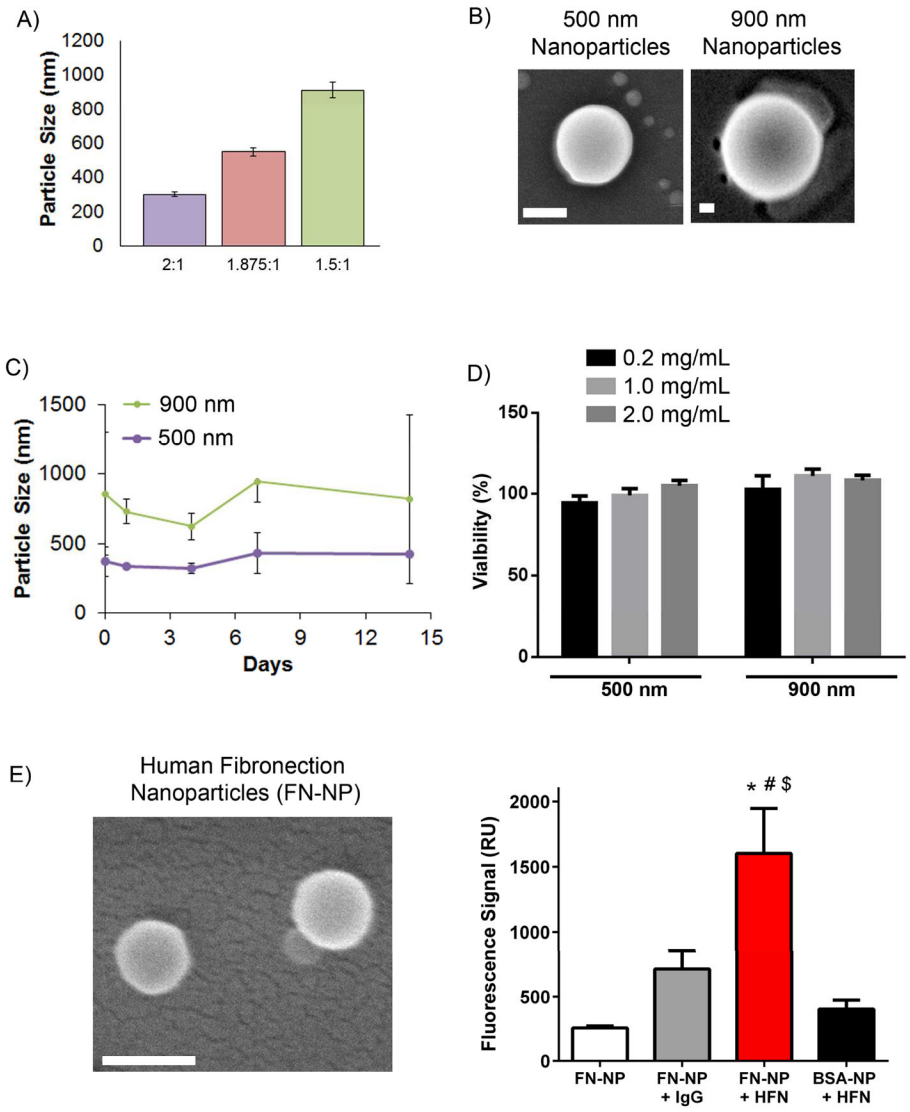

Figure 2. Nanoparticle characterization and cytocompatibility

A) Dynamic light scattering sizing of nanoparticles, measured using the refractive index for water (1.33). B) Scanning electron microscopy (SEM) images of nanoparticles. Scale: 200 nm. C) Particle stability in 1% serum conditions. D) Metabolic activity assay for cytotoxicity for cells incubated with increasing dose of nanoparticles. E) SEM images of Fibronectin nanoparticles (FN-NP, Scale: 200 nm) and the functional ability of resulting FN-NPs in binding to HFN antibody. ANOVA $p<0.0001$; Pairwise: FN-NP + HFN vs. FN-NP: $p<0.001$; FN-NP + HFN vs. FN-NP: $p<0.001$; FN-NP + HFN vs. FN-NP + IgG: $p<0.01$; FN-NP + HFN vs. BSA-NP + HFN: $p<0.001$.

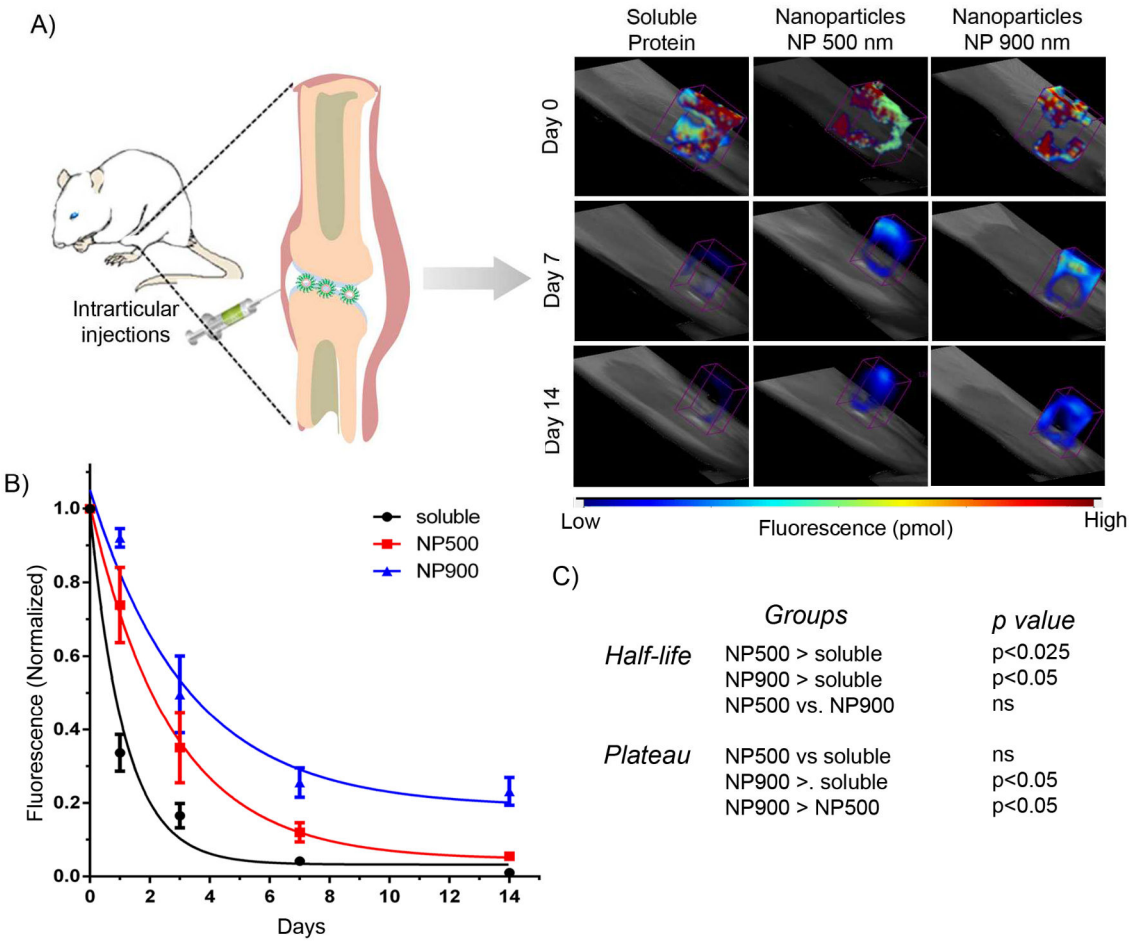

Figure 3. Nanoparticle size controls retention in the intra-articular space in rat joints

A) Fluorescence molecular tomography of rat stifle joint injected with bolus VivoTag®-S 750-BSA protein and nanoparticle-complexed protein. B) VivoTag®-S 750-BSA-particles with 900 nm size show sustained signal compared to 500 nm nanoparticles and soluble BSA. Photon counts were measured in each rat over 14 days by a FMT imaging system and normalized to day 0 photon count for respective rat. The normalized data were fitted using a one-phase exponential decay. C) Statistics representing comparison of nanoparticles and soluble protein. Half-life: NP500 > soluble, $p<0.025$; NP900 > soluble, $p < 0.005$; Plateau: NP900 > soluble, $p < 0.05$; NP900 > NP500, $p <0.05$.